Original Article

# Native $T_1$ mapping for non-invasive quantitative evaluation of renal function and renal fibrosis in patients with chronic kidney disease

**Chao-Gang Wei[1#], Ying Zeng[2#], Rui Zhang[1#], Ye Zhu[2], Jian Tu[3], Peng Pan[1], Qing Ma[1], Lan-Yi Wei[1], Wen-Lu Zhao[1], Jun-Kang Shen[1]**

[1]Department of Radiology, The Second Affiliated Hospital of Soochow University, Suzhou, China; [2]Department of Nephrology, The Second Affiliated Hospital of Soochow University, Suzhou, China; [3]Department of Pathology, The Second Affiliated Hospital of Soochow University, Suzhou, China

*Contributions:* (I) Conception and design: JK Shen, CG Wei; (II) Administrative support: JK Shen, WL Zhao; (III) Provision of study materials or patients: Y Zeng, Y Zhu, J Tu; (IV) Collection and assembly of data: R Zhang; (IV) Data analysis and interpretation: R Zhang, P Pan, Q Ma, LY Wei; (V) Manuscript writing: All authors; (VI) Final approval of manuscript: All authors.

[#]These authors contributed equally to this work.

*Correspondence to:* Jun-Kang Shen, MM; Wen-Lu Zhao, MM. Department of Radiology, The Second Affiliated Hospital of Soochow University, 1055 Sanxiang Road, Suzhou 215004, China. Email: shenjunkang@suda.edu.cn; wenluzhao81@163.com.

**Background:** To investigate the role of native $T_1$ mapping in the non-invasive quantitative assessment of renal function and renal fibrosis (RF) in chronic kidney disease (CKD) patients.

**Methods:** A prospective analysis of 71 consecutive patients [no RF (0%): 9 cases; mild RF (<25%): 36 cases; moderate RF (25–50%): 17 cases; severe RF (>50%): 9 cases] who were clinically diagnosed with CKD that was pathologically confirmed and who underwent magnetic resonance imaging (MRI) examination between October 2021 and September 2022 was performed. $T_1$-C (mean cortical $T_1$ value), $T_1$-M (mean medullary $T_1$ value), $\Delta T_1$ (mean corticomedullary difference) and $T_1$% (mean corticomedullary ratio) values were compared. Correlations between $T_1$ parameters and clinical and histopathological values were analyzed. Regression analysis was performed to determine independent predictors of RF. The areas under the receiver operating characteristic curve (AUC) were calculated to assess the diagnostic value of RF.

**Results:** The $T_1$-C, $\Delta T_1$ and $T_1$% values ($P<0.05$) were significantly different in the CKD group, but $T_1$-M was not ($P>0.05$). The $\Delta T_1$ and $T_1$% values showed significant differences in pairwise comparisons among CKD subgroups ($P<0.05$) except for CKD 2 and 3. $\Delta T_1$ and $T_1$% were moderately correlated with the estimated glomerular filtration rate ($\Delta T_1$: $r_s=-0.561$; $T_1$%: $r=-0.602$), serum creatinine ($\Delta T_1$: $r_s=0.591$; $T_1$%: $r_s=0.563$), blood urea nitrogen ($\Delta T_1$: $r_s=0.433$; $T_1$%: $r_s=0.435$) and histopathological score ($\Delta T_1$: $r_s=0.630$; $T_1$%: $r_s=0.658$). $\Delta T_1$ and $T_1$%, but not $T_1$-C, were independent predictors of RF ($P<0.05$). $\Delta T_1$ and $T_1$% were set as –410.07 ms and 0.8222 with great specificity [$\Delta T_1$: 91.7% (77.5–98.2%); $T_1$%: 97.2% (85.5–99.9%)] to identify mild RF and moderate-severe RF. The optimal cutoff values for differentiating severe RF from mild-moderate RF were –343.81 ms ($\Delta T_1$) and 0.8359 ($T_1$%) with high sensitivity [both 100% (66.4–100%)] and specificity [$\Delta T_1$: 90.6% (79.3–96.9%); $T_1$%: 94.3% (84.3–98.8%)].

**Conclusions:** $\Delta T_1$ and $T_1$% overwhelm $T_1$-C for assessment of renal function and RF in CKD patients. $\Delta T_1$ and $T_1$% identify patients with <25% and >50% fibrosis, which can guide clinical decision-making and help to avoid biopsy-related bleeding.

**Keywords:** Prospective study; native $T_1$ mapping; chronic kidney disease (CKD); renal fibrosis; quantitative assessment

Submitted Nov 27, 2022. Accepted for publication May 12, 2023. Published online May 22, 2023.
doi: 10.21037/qims-22-1304
**View this article at:** https://dx.doi.org/10.21037/qims-22-1304

## Introduction

Chronic kidney disease (CKD) has a high prevalence, poor prognosis and incurs high medical costs. CKD is defined as abnormalities of the kidney structure or function that persist for at least three months. This condition has many health implications for individuals. CKD affects nearly 10% of the population worldwide and is often underrecognized by patients and clinicians (1,2). An accurate assessment of renal function is crucial for monitoring disease progression, treatment response and prognosis management for CKD patients. The most commonly used method to assess renal function is the evaluation of the estimated glomerular filtration rate (eGFR), which is calculated using the CKD epidemiology collaboration (CKD-EPI) equation (3). However, studies have shown that CKD-EPI-based eGFR measurement is not accurate for evaluating renal function in CKD patients mainly due to the large variability caused by the formula only based on serum creatinine (Scr) (4). Besides, the eGFR cannot accurately estimate split kidney function, which is often required for the evaluation of patients with CKD (5).

In addition, renal fibrosis (RF) inevitably occurs during the progression of CKD (6). RF, pathologically characterized by glomerulosclerosis and renal interstitial fibrosis, is an important factor leading to renal structural changes and loss of function. The degree of RF is strongly correlated with the CKD prognosis (7,8). Renal biopsy is the current gold standard for diagnosing RF. Unfortunately, invasive renal biopsy has a considerable risk of serious complications (e.g., gross hematuria, perirenal hematoma, arteriovenous fistula, etc.) (9). Hence, a non-invasive method of monitoring renal function and assessing RF would be a valuable tool to diagnose CKD and guide antifibrotic therapy.

Magnetic resonance imaging (MRI) is a non-invasive examination technology and has been widely used for the whole body because it has high contrast in soft tissues and provides radiation-free, multiplanar and multisequence imaging. However, conventional MRI sequences cannot be used to diagnose renal fibrotic diseases. Although gadolinium-based contrast-enhanced MRI sequences can provide fibrotic imaging of the heart, liver and other organs, gadolinium-based contrast agents are associated with RF and potentially nephrotoxicity, which increases the risk of renal insufficiency (10). In recent years, the application of functional MRI has made it possible to visualize complicated pathophysiological changes in the kidney without the use of contrast media. At present, renal functional MRI techniques mainly include diffusion-weighted imaging (DWI), magnetic resonance elastography (MRE), blood oxygenation level-dependent MRI (BOLD-MRI), and arterial spin labeling (ASL). These modalities can reveal characteristics of renal microvascular perfusion, oxygenation, interstitial diffusion and renal stiffness (11-15). Compared with these functional MRI techniques, relatively few studies on renal diseases have used MRI mapping techniques, which comprise the generation of a parametric map from a series of co-registered images with different $T_1$, $T_2$ or $T_2$* relaxation times (16). Unlike normal $T_1$-, $T_2$-, and $T_2$*-weighted images, parametric mapping allows for the quantification and visualization of focal or diffuse diseases. $T_1$ mapping depicts the spin-lattice (longitudinal) relaxation in tissues and the $T_1$ value (ms) of a voxel represents a time constant for recovery, which has been widely applied to quantitatively evaluate myocardial and articular cartilage lesions and iron overload (17). Furthermore, $T_1$ mapping without the administration of a contrast agent, referred to as native $T_1$ mapping, is highly reproducible and sensitive, especially for patients with renal insufficiency or who are allergic to contrast agents (18-20).

The aim of this study was to utilize native $T_1$ mapping to non-invasively monitor renal function and quantitatively assess RF in patients with CKD. We present this article in accordance with the STARD reporting checklist (available at https://qims.amegroups.com/article/view/10.21037/qims-22-1304/rc).

## Methods

### *Subjects*

The study was conducted in accordance with the Declaration of Helsinki (as revised in 2013). This prospective, single-center study was approved by institutional ethics committee of our hospital (No. JD-LK-2022-060-01) and informed

 

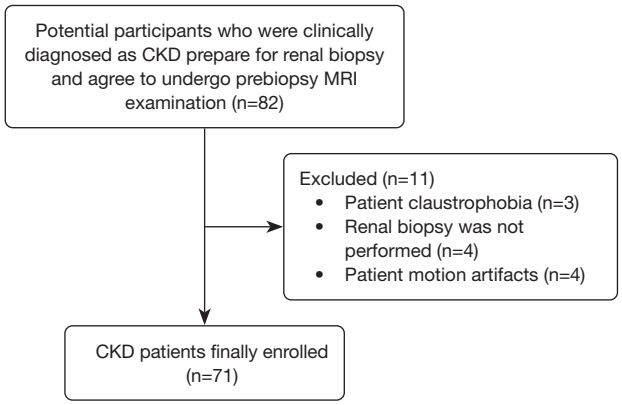


**Figure 1** Flow chart with exclusion criteria of the study participants. CKD, chronic kidney disease; MRI, magnetic resonance imaging.

consent was taken from all the patients. The CKD group comprised 82 patients who were clinically diagnosed with CKD in the Nephrology Department of our tertiary care institution between October 2021 and September 2022 and were prepared for renal biopsy and agreed to undergo prebiopsy MRI examination. Forty healthy volunteers (HVs) with no history of kidney disease, hypertension, diabetes or vascular diseases and had an eGFR ≥90 mL/min/1.73 $m^2$, a Scr and blood urea nitrogen (BUN) level within normal limits, and no proteinuria within 1 year were recruited as the control group. The inclusion criteria for CKD patients were as follows: conformity with a clinical diagnosis of CKD, including a history of proteinuria and/or glomerular hematuria over three months and/or decreased eGRF levels and abnormal kidney-related hematological and biochemical parameters. The MRI examination was performed within 3 days before renal biopsy. After biopsy, the sample underwent histopathological examination. There were no contraindications for MRI. There were no serious diseases of other organs or systems. Participants were excluded from this study for the following conditions: inability to complete the MRI examination due to claustrophobia (n=3), renal biopsy not finally performed (n=4), and no satisfactory MRI images were available for analysis (n=4). A total of 71 consecutive CKD patients were finally enrolled in this study. A flowchart with the exclusion criteria is shown in *Figure 1*.

### *Clinical parameter measurement*

Baseline characteristics, including age, gender, height, weight, body mass index (BMI), blood pressure, and blood glucose were collected for all participants. Hematological and biochemical parameters related to the kidney [Scr, BUN and 24-hour urinary protein (24h-UPRO)] were also collected. No specific 24h-UPRO value could be measured in the HV group due to the lack of proteinuria. The eGFR level was calculated according to the CKD-EPI formula. CKD stages were determined according to the Kidney Disease Outcomes Quality Initiative (K/DOQI) guidelines (1). The clinical and laboratory parameters in the two groups are shown in *Table 1*.

### *MRI acquisition*

MRI of both kidneys was performed with a Prisma 3.0 T scanner (Simens AG, Erlangen, Germany) using an 18-channel total imaging matrix body coil. An identical protocol was used for both the CKD patients and HVs. Native $T_1$ mapping was performed using an end-expiratory, electrocardiographically (ECG)-gated modified Look-Locker inversion recovery (MOLLI) sequence, and breath-holds were used for respiratory motion compensation. MOLLI images of both kidneys were acquired in the coronal plane. The native $T_1$ mapping MRI protocol parameters were as follows: repetition time (TR), 546.6 ms; echo time (TE), 1.1 ms; slice thickness, 5 mm; slice gap, 1 mm; number of slices, 5; field of view, 144 mm × 144 mm; matrix, 290 mm × 290 mm; flip angle, 35°; spatial resolution, 2×2×5 $mm^3$; initial inversion time (TI), 284 ms; TI increment, 80 ms; 10-second breath holds per time. The total time of the sequence was approximately 2 min 47 s.

### *Image analysis*

The reconstruction software (Syngo.via) in the Siemens postprocessing workstation automatically produced a coronary $T_1$ parametric map with pixel-by-pixel computation of the $T_1$ values. The region of interest (ROI) was delineated on the $T_1$ mapping coronary pseudocolor images by two radiologists with similar experience in the urogenital system (reader 1 had 8 years of experience; reader 2 had 10 years of experience) using a double-blind method. For each radiologist, three ROIs were manually drawn at the same symmetrical location of the left and right kidneys, including the superior pole, middle and inferior pole of the cortex and medulla (21). The cortical ROI was set as an oval with an area of 0.14 $cm^2$, while the medullary ROI was circular in shape with an area of 0.18 $cm^2$. The average value of each kidney was taken as the $T_1$ parameter

 

value of that kidney for each radiologist. The final $T_1$ value of each kidney was obtained by averaging the results of the two radiologists. The $T_1$ parameters included the mean cortical $T_1$ value (abbreviated as $T_1$-C), the mean medullary $T_1$ value ($T_1$-M), the mean corticomedullary difference ($\Delta T_1$, $T_1$-C – $T_1$-M) and the mean corticomedullary ratio ($T_1$%, $T_1$-C/$T_1$-M).

### *Renal histopathology*

Ultrasound-guided renal biopsy was performed within 3 days after the MRI examination. Renal biopsies were performed by an experienced pathologist and an experienced nephrologist, who were blinded to the MRI examination results. The patients were kept in the prone position, and a hard sandbag was placed under the abdomen to reduce kidney movement during kidney puncture. In most of the cases, the bottom of the right kidney was the puncture point, 16-gauge needles were used in this study (22). The renal biopsy tissue samples underwent standard histopathological processing. RF was quantitatively evaluated from the kidney biopsy tissue sections by staining them with Masson's trichrome-stain. The evaluation involved assessing the degrees of glomerular injury, tubular interstitial injury and renal atrophy. In addition, according to the proportion of interstitial fibrosis, these patients were classified as no RF (0%), mild RF (<25%), moderate RF (25–50%) and severe RF (>50%) (23).

### *Statistical analysis*

Statistical analyses were performed using SPSS version 22.0 (IBM Corp., Armork, NY, USA) and MedCalc version 15.2.2 (MedCalc Software Ltd., Ostend, Belgium). Graphs were generated using Prism 5 (GraphPad Software Inc., CA, USA). The Kolmogorov-Smirnov test or Shapiro-Wilk test was used for normal distributions. Continuous variables with normal distributions are expressed as mean ± standard deviation (SD). Paired or independent samples *t*-tests and one-way analysis of variance (ANOVA) with Bonferroni correction were used to compare measurements. Continuous variables with a non-normal distribution were analyzed by the Wilcoxon signed-rank test, Mann-Whitney U test or Kruskal-Wallis test and are presented as medians [interquartile range (IQR)]. The interobserver correlation coefficient (ICC) was used to evaluate the variability between the two radiologists. The ICC value ranges from 0 to 1 and was greater than 0.75, indicating good reliability. Correlation analysis between the $T_1$ parameters and clinical and histopathological values was performed by calculating a Pearson (r) or Spearman ($r_s$) correlation coefficient (normality test dependent). The correlation coefficient measures the strength of the relationship between two variables (<0.3, weak correlation; 0.3–0.7, moderate correlation; >0.7, strong correlation) (24). Univariate and multivariate logistic regression models were used to predict RF, and the diagnostic performance of RF was evaluated using a receiver operating characteristic (ROC) curve. Two-tailed P<0.05 indicated statistical significance.

## Results

### *Baseline characteristics of participants*

The baseline characteristics of the 71 CKD patients and 40 HVs enrolled in this study are shown in *Table 1*. All 71 patients underwent renal biopsy and were further classified according to CKD stage (CKD 1: 36 cases; CKD 2: 19 cases; CKD 3: 14 cases; CKD 4: 2 cases) and RF stage (no RF: 9 cases; mild RF: 36 cases; moderate RF: 17 cases; severe RF: 9 cases). There were no significant differences in age, gender, height, weight, BMI, or blood glucose between the CKD and HV groups (P>0.05), but there were significant differences in blood pressure, eGFR, Scr and BUN between the two groups (P<0.05). The major primary causes of CKD in these patients were IgA nephropathy and membranous nephropathy, which together accounted for nearly 68% (48/71) of all cases. The interobserver variability results are shown in *Table 2*. The two radiologists had good reliability for all $T_1$ parameter values for both kidneys, with ICCs greater than 0.75 and P values less than 0.001.

### *Comparison of native $T_1$ mapping parameters in the CKD and HV groups*

In the CKD group, there were no significant differences among any of the native $T_1$ mapping parameters ($T_1$-C, $T_1$-M, $\Delta T_1$ and $T_1$%) between the left and right kidneys, and similar results were found in the HV group (all P>0.05, *Figure 2*). Because there were no significant differences in the $T_1$ parameters between the kidneys, the MRI values of the right (biopsied) kidney were used in this study. As shown in *Table 3*, the $T_1$-C (P=0.003) and $T_1$% (P<0.001) values were significantly longer in the CKD group than in the HV group (right kidney), while no significant difference was

 

**Table 1** Baseline characteristics

| Characteristics | CKD (n=71) | HVs (n=40) | Statistics | P |
|---|---|---|---|---|
| Age (years) | 46 [34, 53] | 41 [34, 49] | −0.990 | 0.322 |
| Gender (male) | 33 (46.5) | 21 (52.5) | 0.371 | 0.542 |
| Height (m) | 1.65±0.09 | 1.70 [1.63, 1.73] | −1.550 | 0.121 |
| Weight (kg) | 65 [56, 77] | 66±12 | −0.240 | 0.811 |
| BMI (kg/m$^2$) | 24.18±3.52 | 22.65 [20.54, 24.57] | −1.849 | 0.064 |
| Blood pressure (hypertension[a]) | 42 (59.2) | 0 (0.0) | 38.065 | <0.001* |
| Blood glucose (mmol/L) | 4.82 [4.55, 5.23] | 4.90 [4.38, 5.10] | −0.522 | 0.602 |
| eGFR (mL/min/1.73 m$^2$) | 87.61±30.47 | 108.70±9.97 | 5.345 | <0.001* |
| Scr (μmol/L) | 76 [57, 109] | 66.5 [55, 79] | −2.411 | 0.016* |
| BUN (mmol/L) | 5.5 [4.2, 6.95] | 4.54±0.97 | −3.128 | 0.002* |
| 24h-UPRO (g/24 h) | 2.12 [0.99, 4.01] | N.A. | N.A. | N.A. |
| CKD stage | | | | |
| 1 (eGFR ≥90) | 36 | N.A. | N.A. | N.A. |
| 2 (eGFR 60–89) | 19 | N.A. | N.A. | N.A. |
| 3 (eGFR 30–59) | 14 | N.A. | N.A. | N.A. |
| 4 (eGFR 15–29) | 2 | N.A. | N.A. | N.A. |
| 5 (eGFR <15) | 0 | N.A. | N.A. | N.A. |
| RF stage | | | | |
| No (0%) | 9 | N.A. | N.A. | N.A. |
| Mild (<25%) | 36 | N.A. | N.A. | N.A. |
| Moderate (25–50%) | 17 | N.A. | N.A. | N.A. |
| Severe (>50%) | 9 | N.A. | N.A. | N.A. |
| Pathological type of CKD | | | | |
| IgA nephropathy | 24 | N.A. | N.A. | N.A. |
| Membranous nephropathy | 24 | N.A. | N.A. | N.A. |
| Minimal change nephropathy | 7 | N.A. | N.A. | N.A. |
| Focal segmental glomerulosclerosis | 4 | N.A. | N.A. | N.A. |
| Hypertensive nephropathy | 4 | N.A. | N.A. | N.A. |
| Lupus nephritis | 3 | N.A. | N.A. | N.A. |
| Diabetic nephropathy | 2 | N.A. | N.A. | N.A. |
| Hepatitis B virus-related nephropathy | 1 | N.A. | N.A. | N.A. |
| Amyloid Nephropathy | 1 | N.A. | N.A. | N.A. |
| Glomerular podocytes | 1 | N.A. | N.A. | N.A. |

Data are presented as mean ± standard deviation, median [interquartile range] or number (%). *, statistically significant; a, hypertension was defined as systolic/diastolic blood pressure ≥140/90 mmHg. CKD, chronic kidney disease; HVs, healthy volunteers; BMI, body mass index; eGFR, estimated glomerular filtration rate; Scr, serum creatinine; BUN, blood urea nitrogen; 24h-UPRO, 24-hour urinary protein; N.A., not applicable.

**Table 2** Interobserver reliability analysis between two radiologists

| Parameters | ICC | P |
|---|---|---|
| Left kidney | | |
| $T_1$-C | 0.904 | <0.001* |
| $T_1$-M | 0.874 | <0.001* |
| $\Delta T_1$ | 0.764 | <0.001* |
| $T_1$% | 0.770 | <0.001* |
| Right kidney | | |
| $T_1$-C | 0.854 | <0.001* |
| $T_1$-M | 0.821 | <0.001* |
| $\Delta T_1$ | 0.792 | <0.001* |
| $T_1$% | 0.797 | <0.001* |

*, statistically significant. $T_1$-C, mean cortical $T_1$ value; $T_1$-M, mean medullary $T_1$ value; $\Delta T_1$, mean corticomedullary difference; $T_1$%, mean corticomedullary ratio; ICC, interobserver correlation coefficient.

evident in $T_1$-M (P=0.283). An increased mean cortical $T_1$ resulted in a significantly reduced $\Delta T_1$ in the CKD group compared with the HV group (P<0.001).

The $T_1$ parameters ($T_1$-C, $\Delta T_1$ and $T_1$%) with statistically significant differences between the CKD and HV group were used for the CKD subgroups analysis, and significant differences were found among the CKD subgroups (all P<0.05, *Table 4*). However, there were no significant differences in the $T_1$-C value between CKD 1 and 2 (P>0.990), 2 and 3 (P=0.074), 3 and 4 (P=0.610). The $\Delta T_1$ and $T_1$% values showed significant differences in all pairwise comparisons except for CKD 2 and 3 (P>0.05, *Figure 3*).

### *Correlation of $T_1$ parameters with clinical and histopathological values*

As shown in *Figure 4*, there were no correlations between $T_1$-C, $\Delta T_1$, $T_1$% and blood pressure (all P>0.05). The $T_1$-C value was negatively correlated with eGFR (r=–0.319, P=0.007) and positively correlated with BUN ($r_s$=0.235, P=0.049), but there was no correlation between $T_1$-C and Scr or 24h-UPRO (P>0.05). The $\Delta T_1$ and $T_1$% values were moderately correlated with eGFR ($\Delta T_1$: $r_s$=–0.561; $T_1$%: r=–0.602), Scr ($\Delta T_1$: $r_s$=0.591; $T_1$%: $r_s$=0.563) and BUN ($\Delta T_1$: $r_s$=0.433; $T_1$%: $r_s$=0.435; all P<0.001). Neither $\Delta T_1$ nor $T_1$% were correlated with the 24h-UPRO (P>0.05). In addition, there were moderate positive correlations between the three $T_1$ parameters and the histopathological scores ($T_1$-C: $r_s$=0.355, P=0.003; $\Delta T_1$: $r_s$=0.630, P<0.001; $T_1$%: $r_s$=0.658, P<0.001).

### *Univariate and multivariate logistic regression models for RF diagnosis*

The native $T_1$ mapping coronary raw images and pseudocolor images of both kidneys in each RF subgroup are shown in *Figure 5*. Univariate logistic regression of patient information, biochemical values and $T_1$ parameters was used to identify significantly different indicators (age, eGFR, $\Delta T_1$, and $T_1$%), which were then used for multivariate binary logistic regression (*Table 5*). Due to multicollinearity between $\Delta T_1$ and $T_1$% ($r_s$=0.945, P<0.001), the strong correlation made it inappropriate for these parameters to be included in the same model. Therefore, two models (Model 1: age + eGFR + $\Delta T_1$; Model 2: age + eGFR + $T_1$%) were used to identify independent predictors for RF. In addition to age, the independent predictors to diagnose RF were $\Delta T_1$ (P=0.028) and $T_1$% (P=0.037).

### *Diagnostic performance of $T_1$ parameters for predicting RF*

ROC curve analysis was used to evaluate the diagnostic value of $\Delta T_1$ and $T_1$% for the prediction of RF. There were no significant differences in AUCs between $\Delta T_1$ and $T_1$% among the no RF *vs.* RF, mild RF *vs.* moderate-severe RF and severe RF *vs.* mild-moderate RF comparisons (*Figure 6*, all P>0.05). As shown in *Table 6*, at the optimal threshold of –474.47 ms, the $\Delta T_1$ value had 66.1% (53.0–77.7%) sensitivity and 88.9% (51.8–99.7%) specificity when comparing no RF with RF. The optimal cutoff for diagnosing RF was set as 0.7829, and the sensitivity and specificity for the $T_1$% value at this threshold were 51.6% (38.6–64.5%) and 100.0% (66.4–100.0%), respectively. When mild RF and moderate-severe RF were compared, the $\Delta T_1$ value was set as –410.07 ms [sensitivity, 61.5% (40.6–79.8%); specificity, 91.7% (77.5–98.2%)] and the $T_1$% value was set as 0.8222 [sensitivity, 53.9% (33.4–73.4%); specificity, 97.2% (85.5–99.9%)]. When comparing severe RF and mild-moderate RF, the optimal cutoff for differentiating them was –343.81 ms for $\Delta T_1$ [sensitivity, 100.0% (66.4–100.0%); specificity, 90.6% (79.3–96.9%)] and 0.8359 for $T_1$% [sensitivity, 100.0% (66.4–100.0%);

 

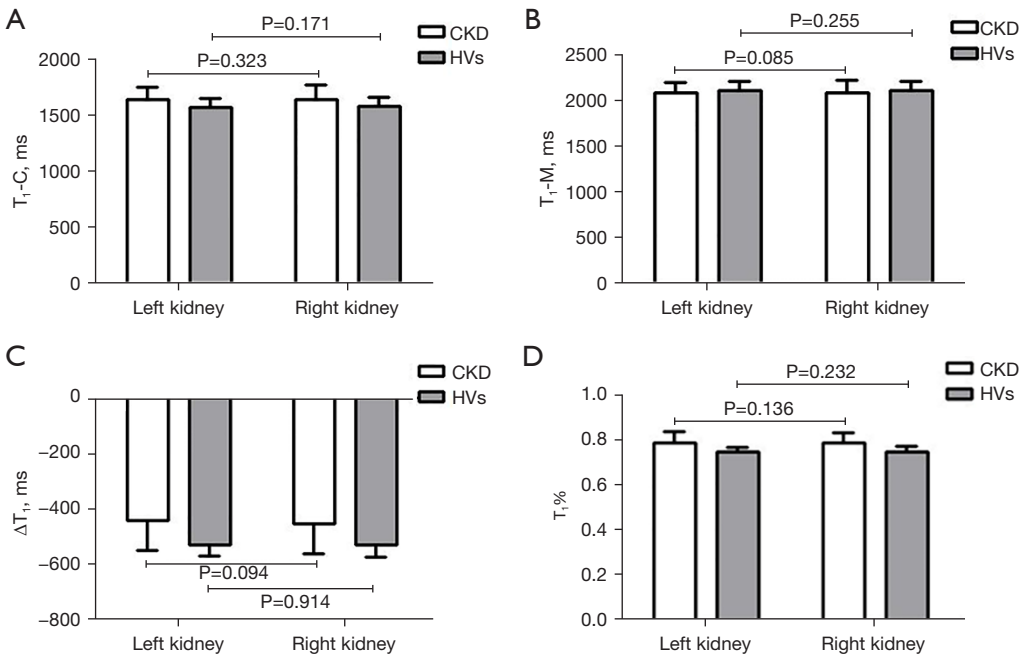


**Figure 2** Comparison of native $T_1$ mapping parameters between both kidneys, including $T_1$-C (A), $T_1$-M (B), $\Delta T_1$ (C) and $T_1$% (D) in both CKD and HVs. $T_1$-C, mean cortical $T_1$ value; $T_1$-M, mean medullary $T_1$ value; $\Delta T_1$, mean corticomedullary difference; $T_1$%, mean corticomedullary ratio. CKD, chronic kidney disease; HVs, healthy volunteers; $T_1$-C, mean cortical $T_1$ value; $T_1$-M, mean medullary $T_1$ value; $\Delta T_1$, mean corticomedullary difference; $T_1$%, mean corticomedullary ratio.

**Table 3** Comparisons of $T_1$ parameters in CKD and HVs groups

| Parameters | Left kidney | | | | Right kidney | | | |
|---|---|---|---|---|---|---|---|---|
| | CKD | HVs | Statistics | P | CKD | HVs | Statistics | P |
| $T_1$-C (ms) | 1,636.56±112.23 | 1,567.89±81.49 | −3.372 | 0.001* | 1,639.96±121.80 | 1,575.31±78.70 | −3.017 | 0.003* |
| $T_1$-M (ms) | 2,078.29±119.99 | 2,104.54±107.51 | 1.148 | 0.254 | 2,085.79±129.66 | 2,111.41±100.69 | 1.079 | 0.283 |
| $\Delta T_1$ (ms) | −441.73±105.78 | −527.47 [−545.64, −505.54] | −5.209 | <0.001* | −452.33 [−514.99, −405.47] | −531.33 [−549.73, −506.95] | −5.123 | <0.001* |
| $T_1$% | 0.7847 [0.7578, 0.8098] | 0.7479 [0.7378, 0.7575] | −5.497 | <0.001* | 0.7870±0.0469 | 0.7499 [0.7357, 0.7568] | −5.374 | <0.001* |

Data are presented as mean ± standard deviation or median [interquartile range]. *, statistically significant. CKD, chronic kidney disease; HVs, healthy volunteers; $T_1$-C, mean cortical $T_1$ value; $T_1$-M, mean medullary $T_1$ value; $\Delta T_1$, mean corticomedullary difference; $T_1$%, mean corticomedullary ratio.

**Table 4** Comparison of significantly-different $T_1$ parameters in CKD stages

| Parameters | CKD 1 (n=36) | CKD 2 (n=19) | CKD 3 (n=14) | CKD 4 (n=2) | Statistics | P |
|---|---|---|---|---|---|---|
| $T_1$-C (ms) | 1,613.68±102.69 | 1,612.81±119.22 | 1,713.83±116.17 | 1,853.61±177.48 | 5.546 | 0.002* |
| $\Delta T_1$ (ms) | −502.29±89.79 | −413.99±73.92 | −381.10±78.38 | −185.18±76.47 | 15.739 | <0.001* |
| $T_1$% | 0.7631±0.0383 | 0.7960±0.0341 | 0.8186±0.0331 | 0.9108±0.0264 | 17.061 | <0.001* |

Data are presented as mean ± standard deviation. *, statistically significant. CKD, chronic kidney disease; $T_1$-C, mean cortical $T_1$ value; $\Delta T_1$, mean corticomedullary difference; $T_1$%, mean corticomedullary ratio.

 

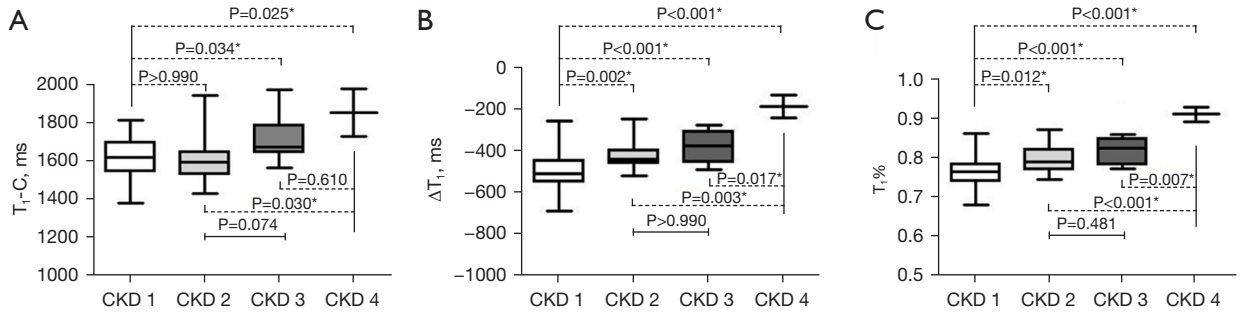


**Figure 3** Pairwise comparisons of native $T_1$ mapping parameters with statistically-different, including $T_1$-C (A), $\Delta T_1$ (B) and $T_1$% (C) in different CKD stages. *, statistically significant. CKD, chronic kidney disease; $T_1$-C, mean cortical $T_1$ value; $\Delta T_1$, mean corticomedullary difference; $T_1$%, mean corticomedullary ratio.

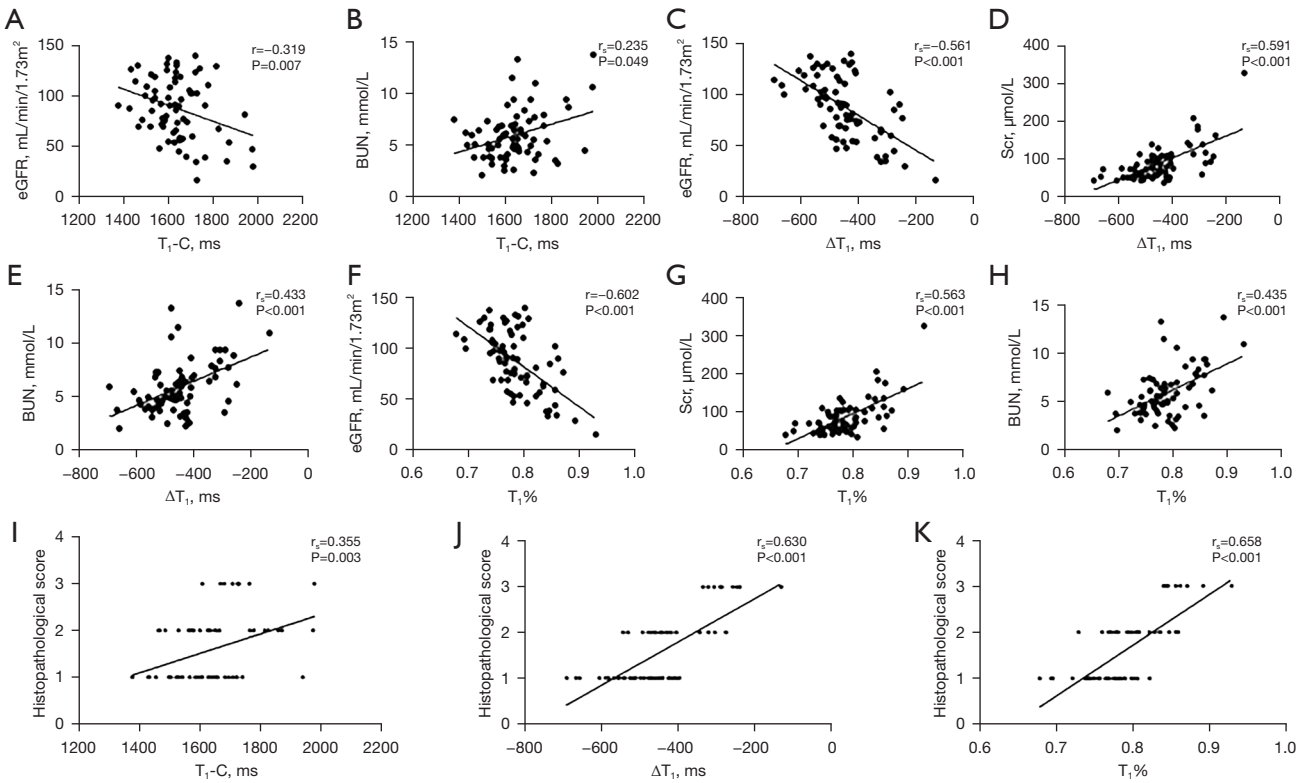


**Figure 4** Pearson or Spearman correlation with statistically-different between the three $T_1$ parameters ($T_1$-C, $\Delta T_1$, $T_1$%) and clinical, histopathological values. Indicators without statistical correlation were not shown in here. (A,B) A mild or moderate correlation of $T_1$-C with eGFR and BUN. (C-E) Moderate correlation between $\Delta T_1$ and eGFR, Scr, BUN. (F-H) Moderate correlation between $T_1$% and eGFR, Scr, BUN. (I-K) moderate positive correlation of $T_1$-C, $\Delta T_1$, $T_1$% with histopathological scores. $T_1$-C, mean cortical $T_1$ value; $\Delta T_1$, mean corticomedullary difference; $T_1$%, mean corticomedullary ratio; eGFR, estimated glomerular filtration rate; Scr, serum creatinine; BUN, blood urea nitrogen.

specificity, 94.3% (84.3–98.8%)]. We also analyzed the different degrees of RF. Overall, there were significant differences among mild, moderate and severe RF ($\Delta T_1$: F=23.785; $T_1$%: F=29.665, P<0.001). In addition, the $\Delta T_1$ and $T_1$% values were significantly different in all pairwise comparisons (*Figure 7*, all P<0.05).

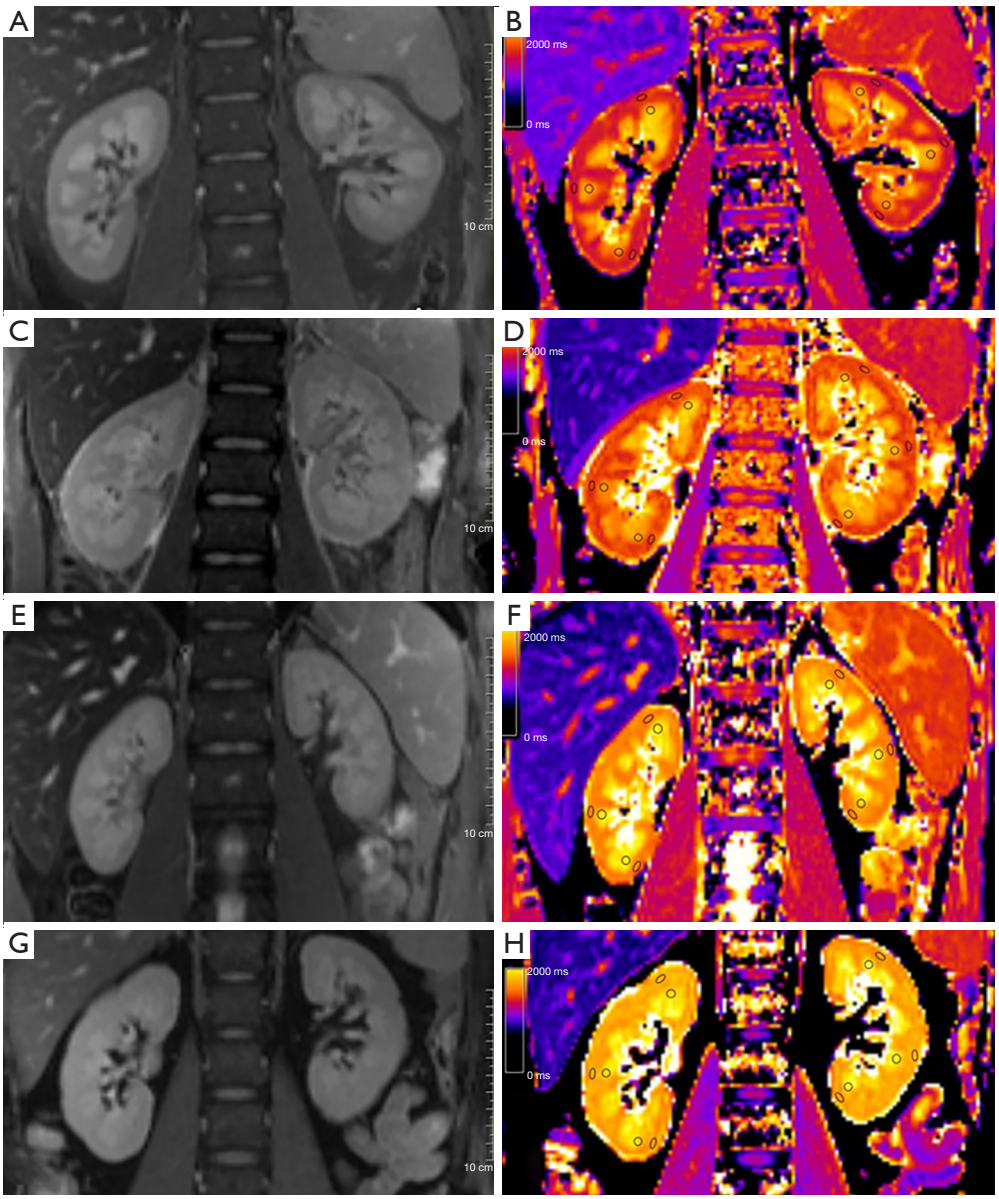


**Figure 5** Native $T_1$ mapping coronary raw images and pseudocolor images of both kidneys in RF subgroups, including no RF (A,B, 0% fibrosis), mild RF (C,D, <25% fibrosis), moderate RF (E,F, 25–50% fibrosis) and severe RF (G,H, >50% fibrosis). Three ROIs were manually drawn at the same symmetrical location of the left and right kidneys, including the superior pole, middle and inferior pole of the cortex and medulla. The cortical ROI was set as oval with an area of 0.14 $cm^2$, while the medullary ROI was circular in shape with an area of 0.18 $cm^2$. RF, renal fibrosis; ROI, region of interest.

## Discussion

Although native $T_1$ mapping has been widely studied in myocardial and liver fibrosis, few studies have assessed $T_1$ mapping in the context of RF. In our study, four $T_1$ parameters, $T_1$-C, $T_1$-M, $\Delta T_1$ and $T_1$%, were used to non-invasively evaluate renal function in CKD patients and to quantitatively assess RF. Similar investigations were previously reported by Berchtold *et al.* (25), Wu *et al.* (26) and Buchanan *et al.* (27). However, all of those studies had a smaller sample size of renal biopsy-proven native CKD patients, and none investigated the role of $T_1$% in CKD and RF. In the present study, we found that the $T_1$-

 

**Table 5** Univariate and multivariate analysis for the diagnosis of renal fibrosis

| Variables | Univariate logistic regression | | Multivariate logistic regression (Model 1) | | Multivariate logistic regression (Model 2) | |
|---|---|---|---|---|---|---|
| | OR (95% CI) | P | OR (95% CI) | P | OR (95% CI) | P |
| Age | 1.085 (1.013–1.163) | 0.020* | 1.107 (1.013–1.211) | 0.025* | 1.087 (1.005–1.175) | 0.037* |
| Gender | 0.659 (0.161–2.690) | 0.561 | N.A. | N.A. | N.A. | N.A. |
| BMI | 0.916 (0.750–1.119) | 0.388 | N.A. | N.A. | N.A. | N.A. |
| Blood pressure | 1.731 (0.423–7.077) | 0.445 | N.A. | N.A. | N.A. | N.A. |
| Blood glucose | 1.710 (0.639–4.577) | 0.286 | N.A. | N.A. | N.A. | N.A. |
| eGFR | 0.973 (0.946–1.001) | 0.048* | 1.007 (0.969–1.046) | 0.715 | 1.000 (0.966–1.036) | 0.985 |
| Scr | 1.010 (0.988–1.032) | 0.376 | N.A. | N.A. | N.A. | N.A. |
| BUN | 1.079 (0.791–1.472) | 0.631 | N.A. | N.A. | N.A. | N.A. |
| 24h-UPRO | 0.834 (0.718–0.968) | 0.183 | N.A. | N.A. | N.A. | N.A. |
| $T_1$-C | 1.005 (0.998–1.012) | 0.142 | N.A. | N.A. | N.A. | N.A. |
| $T_1$-M | 0.998 (0.993–1.004) | 0.499 | N.A. | N.A. | N.A. | N.A. |
| $\Delta T_1$ | 1.011 (1.002–1.020) | 0.016* | 1.013 (1.001–1.025) | 0.028* | N.A. | N.A. |
| $T_1$% | 1.742E+11 (142.937, 2.124E+20) | 0.015* | N.A. | N.A. | 8.306E+10 (4.585, 1.505E+21) | 0.037* |

Model 1: age + eGFR + $\Delta T_1$; Model 2: age + eGFR + $T_1$%. *, statistically significant. BMI, body mass index; eGFR, estimated glomerular filtration rate; Scr, serum creatinine; BUN, blood urea nitrogen; 24h-UPRO, 24-hour urinary protein; $T_1$-C, mean cortical $T_1$ value; $T_1$-M, mean medullary $T_1$ value; $\Delta T_1$, mean corticomedullary difference; $T_1$%, mean corticomedullary ratio; OR, odds ratio; CI, confidence interval; N.A., not applicable.

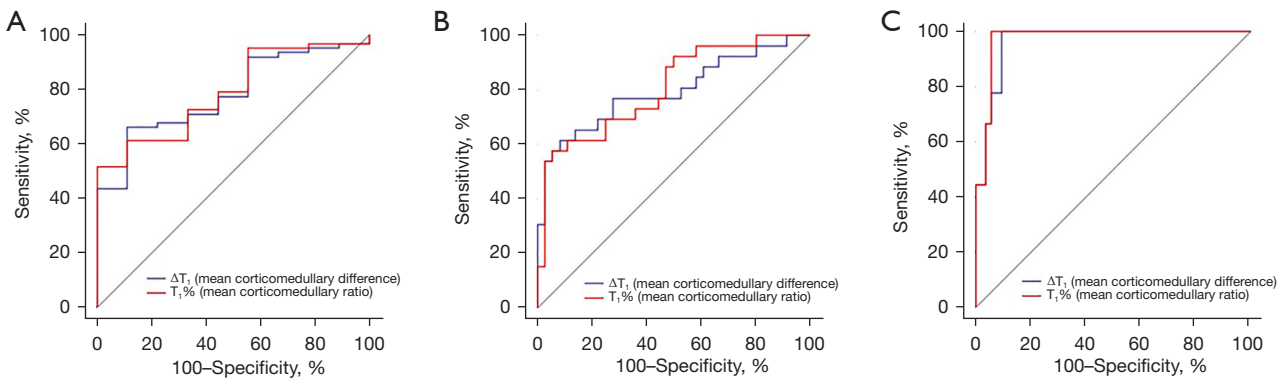


**Figure 6** Comparison of $\Delta T_1$ and $T_1$% in the AUC in different situations. (A) The AUC of $\Delta T_1$ (blue) and $T_1$% (red) for comparison of no RF and RF was 0.781 and 0.789. (B) The AUC of $\Delta T_1$ and $T_1$% for comparison of mild RF and moderate-severe RF was 0.795 and 0.806. (C) The AUC of $\Delta T_1$ and $T_1$% for comparison of severe RF and mild-moderate RF was 0.964 and 0.973. AUC, area under the receiver operating characteristic curve; RF, renal fibrosis; $\Delta T_1$, mean corticomedullary difference; $T_1$%, mean corticomedullary ratio.

C, $\Delta T_1$ and $T_1$% values could be used to help diagnose CKD. Compared with HVs, the CKD group showed a significant increase in $T_1$-C, a significant decrease in $\Delta T_1$ and no significant change in $T_1$-M, which was in accordance with previous studies (27,28). Most studies have focused on the effect of the cortical $T_1$ value and corticomedullary differences on CKD and RF, and no related studies on the corticomedullary ratio ($T_1$%) have been reported thus far.

 

**Table 6** Diagnostic values of $T_1$ parameters for the presence and degree of renal fibrosis

| Parameters | No RF & RF (n=9 & n=62) | | | | Mild RF & moderate-severe RF (n=36 & n=26) | | | | Mild-moderate RF& severe RF (n=53 & n=9) | | | |
|---|---|---|---|---|---|---|---|---|---|---|---|---|
| | AUC (95% CI) | Cutoff | Se (95% CI) | Sp (95% CI) | AUC (95% CI) | Cutoff | Se (95% CI) | Sp (95% CI) | AUC (95% CI) | Cutoff | Se (95% CI) | Sp (95% CI) |
| $\Delta T_1$ (ms) | 0.781 (0.667–0.871) | −474.47 | 66.1 (53.0–77.7) | 88.9 (51.8–99.7) | 0.795 (0.673–0.887) | −410.07 | 61.5 (40.6–79.8) | 91.7 (77.5–98.2) | 0.964 (0.883–0.995) | −343.81 | 100.0 (66.4–100.0) | 90.6 (79.3–96.9) |
| $T_1$% | 0.789 (0.675–0.876) | 0.7829 | 51.6 (38.6–64.5) | 100.0 (66.4–100.0) | 0.806 (0.685–0.895) | 0.8222 | 53.9 (33.4–73.4) | 97.2 (85.5–99.9) | 0.973 (0.896–0.998) | 0.8359 | 100.0 (66.4–100.0) | 94.3 (84.3–98.8) |

RF, renal fibrosis; AUC, the area under the receiver operating characteristic curve; Se, sensitivity; Sp, specificity; CI, confidence interval; $\Delta T_1$, mean corticomedullary difference; $T_1$%, mean corticomedullary ratio.

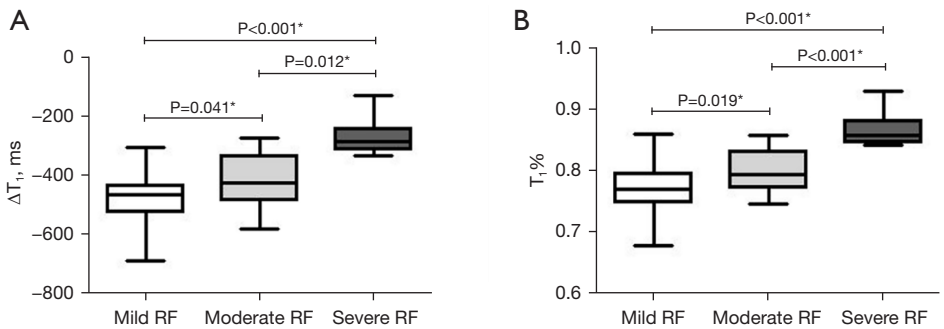


**Figure 7** Pairwise comparisons of $\Delta T_1$ (A) and $T_1$% (B) in between mild RF, moderate RF and severe RF. Both $\Delta T_1$ and $T_1$% values showed statistically-significant differences in any pairwise comparisons (all P<0.05). *, statistically significant. $\Delta T_1$, mean corticomedullary difference; $T_1$%, mean corticomedullary ratio; RF, renal fibrosis.

We found that $T_1$% was higher in the CKD group than in the HV group, mainly due to a significant increase in the cortical $T_1$ value, which was caused by extracellular fluid due to interstitial edema, inflammation or fibrosis (27).

With the exception of $T_1$-M, the other three $T_1$ parameters ($T_1$-C, $\Delta T_1$ and $T_1$%) could be used for evaluating the CKD stage. We found that an increased $T_1$-C and $T_1$%, but a decreased $\Delta T_1$, were associated with a higher CKD stage, with a good correlation between these three parameters and renal function. However, there were no obvious differences in the $T_1$-C value between CKD 1 and 2, 2 and 3, 3 and 4. Unlike $T_1$-C, the $\Delta T_1$ and $T_1$% values showed significant differences in the pairwise comparisons between each CKD subgroup, except for between CKD 2 and 3. These results indicated that $\Delta T_1$ and $T_1$% were better than $T_1$-C for assessing renal function in CKD patients. In the CKD group, $T_1$-C, $\Delta T_1$ and $T_1$% had mild-to-moderate correlations with eGFR, BUN and Scr. In addition, these three $T_1$ parameters showed moderate positive correlations with the histopathological score. Similar results were reported by Wu *et al.* (26). They concluded that cortical $T_1$ could be used for CKD staging and the cortical $T_1$ value was positively correlated with the pathological score. Buchanan *et al.* also reported moderate negative correlations between cortical $T_1$, $\Delta T_1$ and eGFR (27).

We further investigated the role of $T_1$ parameters in the quantitative assessment of RF. All 71 CKD patients were pathologically confirmed by right kidney biopsy and stratified into four RF subgroups (no RF, mild RF, moderate RF and severe RF). The univariate and multivariate logistic regression analyses showed that $\Delta T_1$, but not $T_1$-C, was an independent predictor for the diagnosis of RF in addition to patient age. Our results were similar to the study reported by Berchtold *et al.* (25), but inconsistent with Wu's study (26). Although fibrosis usually affects the renal cortex, the $T_1$-C value varied widely among individuals, ranging from 1,400 to 1,750 ms in our study. The $\Delta T_1$ value generated by comparing the cortex with the medulla could effectively reduce the difference. We also found that the $\Delta T_1$ value became significantly reduced with a higher degree of RF. Interestingly, the $T_1$% value was an independent factor of RF prediction, which may be explained by the same reason

 

as for $\Delta T_1$. These cortex-related values (like $\Delta T_1$ and $T_1$%) weakened the difference among individuals, which helped to better observe RF-associated changes. The diagnostic performances of $\Delta T_1$ and $T_1$% were separately analyzed for differentiating no RF (0%) from RF, mild RF (<25%) from moderate-severe RF, and mild-moderate RF from severe RF (>50%). We found that $\Delta T_1$ and $T_1$% could distinguish the RF subgroups when appropriate thresholds were set. They could identify patients with >50% fibrosis with high sensitivity ($\Delta T_1$:100.0%; $T_1$%: 100.0%) and specificity ($\Delta T_1$:90.6%; $T_1$%: 94.3%). This ability would help to avoid biopsies that carry a risk of serious bleeding in the late stage of RF. In addition, the $\Delta T_1$ and $T_1$% values were also able to identify patients with <25% fibrosis with good sensitivity ($\Delta T_1$: 61.5%; $T_1$%: 53.9%) and high specificity ($\Delta T_1$: 91.7%; $T_1$%: 97.2%), which would contribute to detecting early-stage RF and might help in developing effective treatments to slow RF progression. Our results demonstrated that $\Delta T_1$ and $T_1$% generated by native $T_1$ mapping could be used to non-invasively and quantitatively evaluate renal function and RF in CKD patients.

In our study, the commonly used MOLLI sequence was used to perform renal native $T_1$ mapping without the application of contrast media, which could ensure accurate $T_1$ measurements with high spatial resolution and within a single breath-hold. Renal native $T_1$ mapping with the MOLLI sequence has previously shown satisfactory reproducibility in HVs and diabetic nephropathy patients (19). Recently, magnetic resonance fingerprinting (MRF) was established for relaxation mapping in the kidney. Compared with conventional MOLLI, similar accuracy and precision were achieved using an EPI-based MRF method to quantify the $T_1$ time in the kidneys (29). However, additional studies are needed to explore the application of kidney MRF in routine clinical practice. In addition, renal imaging segmentation is an important step to derive the contours of the kidney, renal cortex and medulla. While manual delineation is currently still considered the gold standard for evaluating kidney segmentation, it is time-consuming, operator dependent and not sufficiently accurate. In our study, some ways may have mitigated the drawbacks of manual methods, the ROI delineation was independently performed by two radiologists, and the ROIs were plotted and averaged at multiple points for both the renal cortex and medulla. In addition, due to the subjective nature of manual methods, the effects of interobserver variability need to be quantified. Our results demonstrated good reliability for all $T_1$ parameters for both kidneys, with ICCs all greater than 0.75 (ranging from 0.764 to 0.904).

There were several limitations to this study. First, this was a monocenter study. Despite the relatively large number of biopsy-proven native CKD patients included, there may have been patient selection bias. Multicenter studies with a larger sample size should be further conducted to validate our results. Second, we manually delineated the ROIs of the bilateral kidneys to obtain corresponding cortical and medullary $T_1$ values. Although manual ROI selection of the renal cortex and medulla is considered to be an acceptable method for image analysis (30), automated ROIs selection is preferred over manual ROI selection. Furthermore, the automatic segmentation of renal cortical and medullary ROIs using artificial intelligence will be investigated our future study. Third, the primary etiology of CKD was not studied. In our study, IgA nephropathy and membranous nephropathy were the major primary causes of CKD. We will enlarge the sample size for an in-depth analysis in a future study.

In conclusion, the promising technology of renal native $T_1$ mapping can be used for the non-invasive diagnosis and quantitative evaluation of CKD and RF. The $\Delta T_1$ and $T_1$% values generated by native $T_1$ mapping were more important than the cortical $T_1$ value when quantitatively evaluating renal function and RF in patients with CKD. $\Delta T_1$ and $T_1$% could identify patients with >50% fibrosis and <25% fibrosis, which would contribute to avoiding biopsy in late-stage RF and could help guide physicians when making decision in early-stage RF in CKD patients.

## Acknowledgments

We thank AJE Editing Service for editing this manuscript.
*Funding:* This work was financially supported by the Suzhou Science and Technology Bureau Development Plan (Grant No. SYS2020147), the National Natural Science Foundation of China (Grant No. 81801754) and the Project of State Key Laboratory of Radiation Medicine and Protection, Soochow University (Grant No. GZK1202023).

## Footnote

*Reporting Checklist:* The authors have completed the STARD reporting checklist. Available at https://qims.amegroups.com/article/view/10.21037/qims-22-1304/rc

*Conflicts of Interest:* All authors have completed the ICMJE uniform disclosure form (available at https://qims.

 

amegroups.com/article/view/10.21037/qims-22-1304/coif). The authors have no conflicts of interest to declare.

*Ethical Statement:* The authors are accountable for all aspects of the work in ensuring that questions related to the accuracy or integrity of any part of the work are appropriately investigated and resolved. The study was conducted in accordance with the Declaration of Helsinki (as revised in 2013). This prospective, single-center study was approved by institutional ethics committee of our hospital (No. JD-LK-2022-060-01) and informed consent was taken from all the patients.



## References

1. Stevens PE, Levin A; . Evaluation and management of chronic kidney disease: synopsis of the kidney disease: improving global outcomes 2012 clinical practice guideline. Ann Intern Med 2013;158:825-30.
2. Global, regional, and national burden of chronic kidney disease, 1990-2017: a systematic analysis for the Global Burden of Disease Study 2017. Lancet 2020;395:709-33.
3. Levey AS, Stevens LA, Schmid CH, Zhang YL, Castro AF 3rd, Feldman HI, Kusek JW, Eggers P, Van Lente F, Greene T, Coresh J; . A new equation to estimate glomerular filtration rate. Ann Intern Med 2009;150:604-12.
4. Porrini E, Ruggenenti P, Luis-Lima S, Carrara F, Jiménez A, de Vries APJ, Torres A, Gaspari F, Remuzzi G. Estimated GFR: time for a critical appraisal. Nat Rev Nephrol 2019;15:177-90.
5. Shi W, Liang X, Wu N, Zhang H, Yuan X, Tan Y. Assessment of Split Renal Function Using a Combination of Contrast-Enhanced CT and Serum Creatinine Values for Glomerular Filtration Rate Estimation. AJR Am J Roentgenol 2020;215:142-7.
6. Liu Y. Renal fibrosis: new insights into the pathogenesis and therapeutics. Kidney Int 2006;69:213-7.
7. Berchtold L, Friedli I, Vallée JP, Moll S, Martin PY, de Seigneux S. Diagnosis and assessment of renal fibrosis: the state of the art. Swiss Med Wkly 2017;147:w14442.
8. Liu Y. Cellular and molecular mechanisms of renal fibrosis. Nat Rev Nephrol 2011;7:684-96.
9. Xu S, Ma L, Lin J, Zhang Z, Wang X, Yin J. Efficacy and safety of percutaneous renal biopsy performed using 18G needle versus 16G needle: a single-center retrospective study. Int Urol Nephrol 2022;54:3255-61.
10. Rudnick MR, Wahba IM, Leonberg-Yoo AK, Miskulin D, Litt HI. Risks and Options With Gadolinium-Based Contrast Agents in Patients With CKD: A Review. Am J Kidney Dis 2021;77:517-28.
11. Sigmund EE, Vivier PH, Sui D, Lamparello NA, Tantillo K, Mikheev A, Rusinek H, Babb JS, Storey P, Lee VS, Chandarana H. Intravoxel incoherent motion and diffusion-tensor imaging in renal tissue under hydration and furosemide flow challenges. Radiology 2012;263:758-69.
12. Xu X, Fang W, Ling H, Chai W, Chen K. Diffusion-weighted MR imaging of kidneys in patients with chronic kidney disease: initial study. Eur Radiol 2010;20:978-83.
13. Li J, An C, Kang L, Mitch WE, Wang Y. Recent Advances in Magnetic Resonance Imaging Assessment of Renal Fibrosis. Adv Chronic Kidney Dis 2017;24:150-3.
14. Li LP, Tan H, Thacker JM, Li W, Zhou Y, Kohn O, Sprague SM, Prasad PV. Evaluation of Renal Blood Flow in Chronic Kidney Disease Using Arterial Spin Labeling Perfusion Magnetic Resonance Imaging. Kidney Int Rep 2017;2:36-43.
15. Morrell GR, Zhang JL, Lee VS. Magnetic Resonance Imaging of the Fibrotic Kidney. J Am Soc Nephrol 2017;28:2564-70.
16. Wolf M, de Boer A, Sharma K, Boor P, Leiner T, Sunder-Plassmann G, Moser E, Caroli A, Jerome NP. Magnetic resonance imaging T1- and T2-mapping to assess renal structure and function: a systematic review and statement paper. Nephrol Dial Transplant 2018;33:ii41-50.
17. Messroghli DR, Moon JC, Ferreira VM, Grosse-Wortmann L, He T, Kellman P, Mascherbauer J, Nezafat R, Salerno M, Schelbert EB, Taylor AJ, Thompson R, Ugander M, van Heeswijk RB, Friedrich MG. Clinical recommendations for cardiovascular magnetic resonance mapping of T1, T2, T2* and extracellular volume: A consensus statement by the Society for Cardiovascular Magnetic Resonance (SCMR) endorsed by the European Association for Cardiovascular Imaging (EACVI). J Cardiovasc Magn Reson 2017;19:75.
18. Graham-Brown MP, Rutherford E, Levelt E, March DS, Churchward DR, Stensel DJ, McComb C, Mangion K,

 

Cockburn S, Berry C, Moon JC, Mark PB, Burton JO, McCann GP. Native T1 mapping: inter-study, inter-observer and inter-center reproducibility in hemodialysis patients. J Cardiovasc Magn Reson 2017;19:21.
19. Dekkers IA, Paiman EHM, de Vries APJ, Lamb HJ. Reproducibility of native T(1) mapping for renal tissue characterization at 3T. J Magn Reson Imaging 2019;49:588-96.
20. Graham-Brown MP, Singh A, Wormleighton J, Brunskill NJ, McCann GP, Barratt J, Burton JO, Xu G. Association between native T1 mapping of the kidney and renal fibrosis in patients with IgA nephropathy. BMC Nephrol 2019;20:256.
21. Zhao J, Wang ZJ, Liu M, Zhu J, Zhang X, Zhang T, Li S, Li Y. Assessment of renal fibrosis in chronic kidney disease using diffusion-weighted MRI. Clin Radiol 2014;69:1117-22.
22. Xu J, Wu X, Xu Y, Ren H, Wang W, Chen W, Shen P, Li X, Shi H, Xie J, Chen X, Zhang W, Pan X. Acute Kidney Disease Increases the Risk of Post-Kidney Biopsy Bleeding Complications. Kidney Blood Press Res 2020;45:873-82.
23. Srivastava A, Palsson R, Kaze AD, Chen ME, Palacios P, Sabbisetti V, Betensky RA, Steinman TI, Thadhani RI, McMahon GM, Stillman IE, Rennke HG, Waikar SS. The Prognostic Value of Histopathologic Lesions in Native Kidney Biopsy Specimens: Results from the Boston Kidney Biopsy Cohort Study. J Am Soc Nephrol 2018;29:2213-24.
24. Ratner B. The correlation coefficient: its values range between +1/-1, or do they? Journal of Targeting, Measurement and Analysis for Marketing 2009;17:139-42.
25. Berchtold L, Friedli I, Crowe LA, Martinez C, Moll S, Hadaya K, de Perrot T, Combescure C, Martin PY, Vallée JP, de Seigneux S. Validation of the corticomedullary difference in magnetic resonance imaging-derived apparent diffusion coefficient for kidney fibrosis detection: a cross-sectional study. Nephrol Dial Transplant 2020;35:937-45.
26. Wu J, Shi Z, Zhang Y, Yan J, Shang F, Wang Y, Lu H, Gu H, Dou W, Wang X, Yuan L. Native T1 Mapping in Assessing Kidney Fibrosis for Patients With Chronic Glomerulonephritis. Front Med (Lausanne) 2021;8:772326.
27. Buchanan CE, Mahmoud H, Cox EF, McCulloch T, Prestwich BL, Taal MW, Selby NM, Francis ST. Quantitative assessment of renal structural and functional changes in chronic kidney disease using multi-parametric magnetic resonance imaging. Nephrol Dial Transplant 2020;35:955-64.
28. Cox EF, Buchanan CE, Bradley CR, Prestwich B, Mahmoud H, Taal M, Selby NM, Francis ST. Multiparametric Renal Magnetic Resonance Imaging: Validation, Interventions, and Alterations in Chronic Kidney Disease. Front Physiol 2017;8:696.
29. Hermann I, Chacon-Caldera J, Brumer I, Rieger B, Weingärtner S, Schad LR, Zöllner FG. Magnetic resonance fingerprinting for simultaneous renal T(1) and T2* mapping in a single breath-hold. Magn Reson Med 2020;83:1940-8.
30. Dekkers IA, de Boer A, Sharma K, Cox EF, Lamb HJ, Buckley DL, et al. Consensus-based technical recommendations for clinical translation of renal T1 and T2 mapping MRI. MAGMA 2020;33:163-76.

**Cite this article as:** Wei CG, Zeng Y, Zhang R, Zhu Y, Tu J, Pan P, Ma Q, Wei LY, Zhao WL, Shen JK. Native T1 mapping for non-invasive quantitative evaluation of renal function and renal fibrosis in patients with chronic kidney disease. Quant Imaging Med Surg 2023;13(8):5058-5071. doi: 10.21037/qims-22-1304

 